Physics Letters A 376 (2012) 2413–2417

Contents lists available at SciVerse ScienceDirect

Physics Letters A

www.elsevier.com/locate/pla

The DNA electronic specific heat at low temperature: The role of aperiodicity

R.G. Sarmento [a], G.A. Mendes [b], E.L. Albuquerque [b,*], U.L. Fulco [b], M.S. Vasconcelos [c], O. Ujsághy [d], V.N. Freire [e], E.W.S. Caetano [f]

[a] Departamento de Física, Universidade Federal do Rio Grande do Norte, 59072-970, Natal, RN, Brazil
[b] Departamento de Biofísica e Farmacologia, Universidade Federal do Rio Grande do Norte, 59072-970, Natal, RN, Brazil
[c] Escola de Ciências e Tecnologia, Universidade Federal do Rio Grande do Norte, 59072-970, Natal, RN, Brazil
[d] Department of Theoretical Physics and Condensed Matter Research Group of the Hungarian Academy of Sciences, Budapest University of Technology and Economics, Budafoki út 8, H-1521 Budapest, Hungary
[e] Departamento de Física, Universidade Federal do Ceará, 60455-760, Fortaleza, CE, Brazil
[f] Instituto Federal de Educação, Ciência e Tecnologia do Ceará, 60040-531, Fortaleza, CE, Brazil

ARTICLE INFO

Article history:
Received 23 March 2012
Received in revised form 26 April 2012
Accepted 29 May 2012
Available online 1 June 2012
Communicated by R. Wu

Keywords:
DNA molecule
Electronic density of states
Electronic specific heat
Quasiperiodic structures

ABSTRACT

The electronic specific heat spectra at constant volume (C_V) of a long-range correlated extended ladder model, mimicking a DNA molecule, is theoretically analyzed for a stacked array of a double-stranded structure made up from the nucleotides guanine *G*, adenine *A*, cytosine *C* and thymine *T*. The role of the aperiodicity on C_V is discussed, considering two different nucleotide arrangements with increasing disorder, namely the Fibonacci and the Rudin–Shapiro quasiperiodic structures. Comparisons are made for different values of the band fillings, considering also a finite segment of natural DNA, as part of the human chromosome Ch22.

Nowadays there are a lot of interest to investigate the DNA's potential applications in nanoelectronic devices, not only as a template for assembling nanocircuits, but also as an element of such circuits, triggering a series of experimental and theoretical investigations [1–7]. Besides, using a full range of quantum mechanical and biochemical methods, studies on the conformational behavior of DNA-based molecules with periodic/quasiperiodic nucleotide sequences have now established that they are a promising biological medium for the efficient transport of charge carriers (electrons and holes) [8–10].

As the characterization of biomolecules presents a high degree of complexity together with a high level of precision, approximate methods must be used [11,12]. Among them, *ab initio* methods based on solving the quantum mechanical interacting electron–ion problem with no adjustable parameters, emerge as a good candidate to deal with this kind of problem. However, in practice, because of computational demands and fundamental limitations, traditional *ab initio* methods, such as the Hartree–Fock and the correlated wave function approaches, are confined to small molecules, providing a limited database for fitting empirical potential parameters [13]. Fortunately, the development of powerful computer softwares has overcome this problem, allowing their use for a wide range of molecular dynamics simulations (for a review see [14]). Specifically, methods based on Hohenberg–Kohn–Sham density functional theory (DFT) [15–17] in combination with faster (parallel) computers have greatly expanded the range of directly accessible systems. Nevertheless, while electrical conductivity of biological molecules has been extensively studied, their corresponding thermal properties remain largely unexplored.

In a recent paper [18], it was shown that the knowledge of thermal properties, like the specific heat and chemical potential, may be useful to characterize different genetical diseases, such as the neurodegenerative ones (Alzheimer, Parkinson, and Creutzfeldt–Jakob, among them). It is the aim of this work to push this field forward by investigating the thermal properties (the electronic specific heat spectra) of quasiperiodic extended ladder model mimicking a double-strand DNA (ds-DNA) segments, considered as a sequence of four possible nucleotides, namely guanine *G*, adenine *A*, cytosine *C* and thymine *T*, arranged according to the Fibonacci and Rudin–Shapiro quasiperiodic sequences. For comparison we considered a segment of the first sequenced human chromosome 22 (Ch22), whose arrangement was retrieved from the internet page of the National Center of Biotechnology Information. We utilize here the same theoretical model used in Zilly et al. [19] which is based on a tight-binding model and fits well all of the experimental data of Refs. [20–22]. Our main aim is to investigate

* Corresponding author. Tel.: +55 84 32153793; fax: +55 84 32153791.
E-mail address: eudenilson@gmail.com (E.L. Albuquerque).

0375-9601/$ – see front matter
http://dx.doi.org/10.1016/j.physleta.2012.05.058

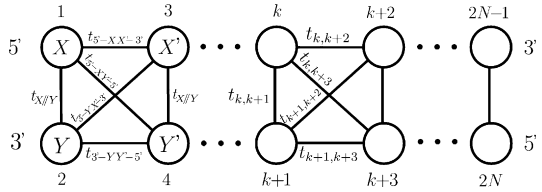

Fig. 1. The extended ladder model to mimic a DNA molecule. Here the letters X, Y, X' and Y' represent the base pairs: guanine, adenine, cytosine, and thymine.

the role of aperiodic order [23] in different electronic specific heat (ESH) spectra profiles, seeking possible differences and similarities among them, with the purpose to establish some kind of standard behavior.

To mimic the DNA molecule, we consider the so-called extended ladder model [19,24,25], as depicted in Fig. 1. It seems to be more appropriate to describe the DNA molecule than the simple ladder model [26], since the diagonal interstrand transfer matrix elements additionally presented in the former are more relevant than the vertical intrastrand coupling [27–29]. Its tight-binding model Hamiltonian is given by:

$$
\begin{aligned}
H = {} & \sum_{j=1}^{2N} \varepsilon_j |j\rangle\langle j| + \sum_{j=1}^{2(N-1)} t_{j,j+2}\big[|j\rangle\langle j+2| + |j+2\rangle\langle j|\big] \\
& + \sum_{j=1}^{N} t_{2j-1,2j}\big[|2j-1\rangle\langle 2j| + |2j\rangle\langle 2j-1|\big] \\
& + \sum_{j=1}^{N-1} \big[t_{2j-1,2j+2}\big(|2j-1\rangle\langle 2j+2| + |2j+2\rangle\langle 2j-1|\big) \\
& + t_{2j,2j+1}\big(|2j\rangle\langle 2j+1| + |2j+1\rangle\langle 2j|\big)\big], \qquad (1)
\end{aligned}
$$

where N is the number of DNA's base pairs, and ε_j is the ionization on-site energy representing the guanine ($j = G$), adenine ($j = A$), cytosine ($j = C$), and thymine ($j = T$) bases, respectively. Also, t, is the nonrandom hopping amplitudes. The long-range on-site energies used here are evaluated by using the density-functional theory (DFT), which depend on the flanking nucleobases [27]. It means that we average the 16 values for the one-site energy given in Ref. [27] for each nucleobases, as it was done in Ref. [19] in which the extended ladder model of DNA was proposed and studied. This yield: $\varepsilon_G = 8.178$, $\varepsilon_A = 8.631$, $\varepsilon_C = 9.722$, and $\varepsilon_T = 9.464$, all units in eV. The hopping parameters are listed in Table 1, where a single-strand sequence notation was used (the other strand is determined considering the DNA unique base pairing). Because of the directionality of DNA strands, $t_{5'-XY-3'} \neq t_{3'-XY-5'} = t_{5'-YX-3'}$ for $X \neq Y$. Furthermore, due to symmetry, $t_{5'-XY-5'} = t_{5'-YX-5'}$, and $t_{3'-XY-3'} = t_{3'-YX-3'}$ for all X, Y.

To setup a quasiperiodic chain of Rudin–Shapiro (RS) type, we consider a G (guanine) base as seed, building the sequence through the inflation rules $G \to GC$, $C \to GA$, $A \to TC$, and $T \to TA$. The RS sequence belongs to the family of the so-called substitutional sequences, which are characterized by the nature of their Fourier spectrum. It exhibits an absolutely continuous Fourier measure, a property which it shares with the random sequences [30]. It should be contrasted with the Fibonacci sequence, which displays a dense pure point Fourier measure, characteristic of a true quasicrystal-like structure (for a review of the physical properties of these and others quasiperiodic structures see Refs. [31,32]). This important difference has been discussed in the literature in connection with the localization properties of both elementary excitations [33] and classical waves [34] in the RS sequence, as compared to other substitutional sequence. The quasiperiodic Fibonacci sequence is constructed starting again from a G (guanine) base as seed and following the inflation rule $G \to GC$, $C \to G$. On the other hand, the first sequenced human chromosome 22 (Ch22) contains about 3.49×10^7 nucleotides, its largest segment (Genbank ID: NT_011520) about 2.33×10^7 nucleotides, and the second largest one about 4.25×10^6 nucleotides. Here, we consider a very short sequence (the maximum number of nucleotides is 512) selected from the largest segment NT_011520 (for a statistical study of this sequence see Ref. [35]), starting also from a G (guanine) base.

Table 1
Hopping parameters for the extended ladder model (all energies are expressed in eV) [19,27].

X	Y			
	G	A	C	T
(a) $t_{5'-XY-3'} = t_{3'-YX-5'}$				
G	0.053	−0.077	−0.114	0.141
A	−0.010	−0.004	0.042	−0.063
C	0.009	−0.002	0.022	−0.055
T	0.018	−0.031	−0.028	0.180
(b) $t_{5'-XY-5'}$				
G	0.012	−0.013	0.002	−0.009
A	−0.013	0.031	−0.001	0.007
C	0.002	−0.001	0.001	0.0003
T	−0.009	0.007	0.0003	0.001
(c) $t_{3'-XY-3'}$				
G	−0.032	−0.011	0.022	−0.014
A	−0.011	0.049	0.017	−0.007
C	0.022	0.017	0.010	−0.004
T	−0.014	−0.007	−0.004	0.006

To evaluate the electronic density of states (DOS) it is necessary to rewrite the Hamiltonian in Eq. (1) in matrix form as:

$$
H = \begin{pmatrix}
\varepsilon_1 & \lambda_{1,2} & t_{1,3} & v_{1,4} & & & & & & \\
\lambda_{1,2} & \varepsilon_2 & v_{2,3} & t_{2,4} & & & & 0 & & \\
t_{1,3} & v_{2,3} & \varepsilon_3 & \lambda_{3,4} & t_{3,5} & v_{3,6} & & & & \\
v_{1,4} & t_{2,4} & \lambda_{3,4} & \varepsilon_4 & v_{4,5} & t_{4,6} & \ddots & & & \\
 & & t_{3,5} & v_{4,5} & \varepsilon_5 & \lambda_{5,6} & \ddots & & & \\
 & & v_{3,6} & t_{4,6} & \lambda_{5,6} & \varepsilon_6 & \ddots & t_{N-3,N-1} & v_{N-3,N} & \\
 & & & \ddots & \ddots & \ddots & \ddots & v_{N-2,N-1} & t_{N-2,N} & \\
 & 0 & & & & t_{N-3,N-1} & \lambda_{N-2,N-1} & \varepsilon_{N-1} & \lambda_{N-1,N} & \\
 & & & & & v_{N-3,N} & t_{N-2,N} & v_{N-1,N} & \varepsilon_N &
\end{pmatrix}. \qquad (2)
$$

Based on Dean's negative eigenvalue theorem [36], the Schrödinger equation can be solved and the eigenvalue can be obtained exactly. The corresponding DOS is written as

$$
\rho(E) = \lim_{N\to\infty} \frac{1}{N} \sum_k \delta(E - E_k). \qquad (3)
$$

Fig. 2 shows the DOS for several intra-strand nucleobases couplings and for several inter-strands ones, taking into account the three different sequences discussed in this Letter: (a) Fibonacci, (b) Rudin–Shapiro and (c) human chromosome 22 (Ch22).

Rather than traces of bands, the DOS profile for each structure is fragmented, showing a number of discrete strongly localized bunches of states that are believed to reflect their 1D band structure. Observe that the number of van Hove singularities is bigger for the RS and Ch22 structures than for the simplest Fibonacci one. Surely this fact will be reflected into the ESH spectra discussed later. Indeed, by inspecting Fig. 2, one can observe that for the Fibonacci case, there are two well-defined regions

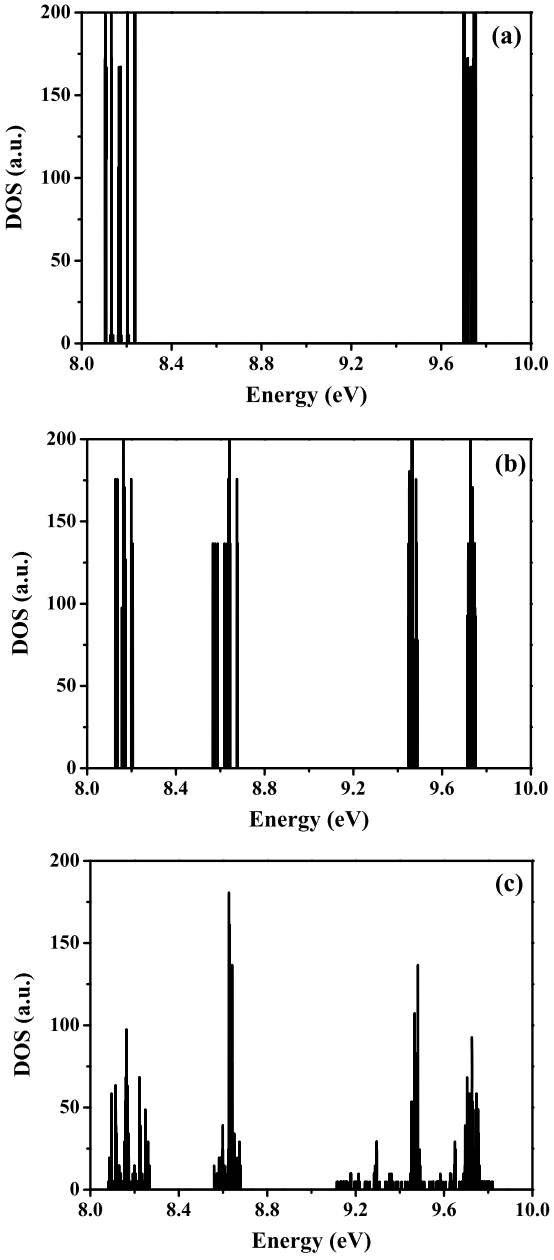

Fig. 2. The electronic density of states (DOS) in arbitrary units plotted against the energy E (in eV) for: (a) Fibonacci sequence; (b) Rudin–Shapiro sequence; (c) DNA human chromosome 22 (Ch22).

around $\varepsilon_G = 8.1$ eV and $\varepsilon_C = 9.7$ eV, respectively. On the other hand, the Rudin–Shapiro and Ch22 structures have four regions centered roughly at the ionization energies of their nucleotides $\varepsilon_G = 8.178$ eV, $\varepsilon_A = 8.631$ eV, $\varepsilon_C = 9.722$ eV, $\varepsilon_T = 9.464$ eV, respectively.

The thermodynamic behavior can be now directly obtained from the above electronic density of states. According to the Fermi–Dirac statistics, the average occupation number of each energy state is given by $f(E) = [1 + \exp[\beta(E-\mu)]]^{-1}$, where $\beta = 1/k_B T$, and μ is the chemical potential. Here, we are not including the spin degeneracy.

The ESH at constant volume is then evaluated by differentiating the average internal energy $U(N_e/N, T)$ with respect to the temperature T, keeping the volume of the system V constant by maintaining fixed the total number of one-particle accessible states N. It is then straightforward to obtain the following expression for the ESH:

$$\frac{C_V}{k_B} = \frac{\beta^2}{4}\left[\sum_n E_n^2 \cosh^{-2} y_n - \frac{(\sum_n E_n \cosh^{-2} y_n)^2}{\sum_n \cosh^{-2} y_n}\right], \tag{4}$$

where $y_n = \beta[(E_n - \mu)/2]$. It is important to mention that in the above expression the chemical potential $\mu = \mu(N_e/N, T)$ can be computed as a function of the temperature and the band filling N_e/N from

$$N_e = \sum_{n=1}^{N} \langle f(E_n) \rangle, \tag{5}$$

and can then be extracted by numerical methods. Here, N_e is the number of non-interacting Fermi particles (electrons), while N is the total number of one-particle accessible states (electrons and holes). The average internal energy can be found from

$$U(N_e/N, T) = \sum_{n=1}^{N} E_n \langle f(E_n) \rangle, \tag{6}$$

where the temperature dependence of the chemical potential $\mu(N_e/N, T)$ is explicitly taken into account. Observe further that in the limit of high temperatures and/or at very low electron densities, the ESH tends to the one obtained through the determination of the partition function using the classical Boltzmann–Gibbs statistics [37].

Fig. 3 depicts a log-log plot of the normalized specific heat spectra at constant volume (in units of the number of non-interacting Fermi particles N_e times the Boltzmann's constant k_B) versus the temperature T for the Fibonacci sequence (solid line), the Rudin–Shapiro sequence (dashed line), and the DNA human chromosome 22 – Ch22 (dotted line). Three values of the band fillings N_e/N are considered, namely $N_e/N = 0.9$ (Fig. 3a), 0.6 (Fig. 3b), and 0.4 (Fig. 3c), for all sequences studied.

Broadly speaking, Fig. 3 shows that an increased disorder (Fibonacci → Rudin–Shapiro → Ch22) gives rise to a structured C_V, with a different band filling N_e/N and temperature T dependence. Although the existence of a structure in the DNA heat capacity at low temperatures has already being demonstrated experimentally, it was strictly assigned to the difference in hydration and/or structural transitions related to the various DNA conformations. Our theoretical/computational analysis indicates that only the C_V behavior of a more disordered nucleotides arrangement can approach that of the human chromosome 22. This last finding supports the visionary and historical idea of Schrödinger [38], in which he predicted that a gene or perhaps a whole chromosome thread represents an aperiodic solid.

Furthermore, at these band fillings ($N_e/N = n/10$, $n = 4, 6, 9$) the Fermi energy falls in a dense region of the energy spectrum. Therefore, there are empty states closer to the ground state, and these can be thermally occupied even at very low temperatures. For a periodic infinite crystal, the energy spectrum yields a linear temperature dependence (in the low-temperature regime) of the ESH. However, although quasiperiodic systems may not being classifiable in the nonlinear physics context, they do exhibit a multifractality in their spectra (see [31,32] for a review) and, instead of the expected linear temperature behavior, the internal energy scales as a power law $U - U_0 \propto T^{1+\phi}$, and consequently $C_v \propto T^{\phi}$. In our case, these ϕ exponents are equal to 0.12 (Fibonacci sequence), 0.15 (Rudin–Shapiro sequence) and 0.23 (Ch22 DNA finite segment), no matter the value of the band fillings N_e/N. This universality class of the specific heat decay exponent at low-temperature, as far as the band fillings N_e/N are concerned, can be understood on basis of a simple multifractal scale argument.

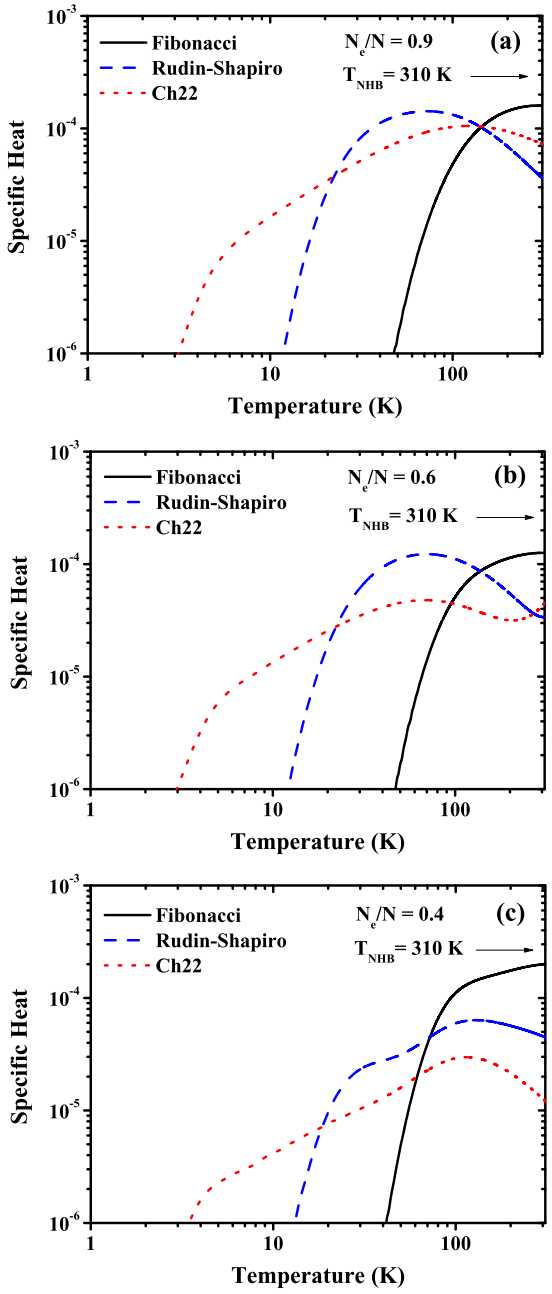

Fig. 3. (Color online.) The log–log plot of the ESH spectra against the energy E (in eV) for the Fibonacci sequence (solid line), the Rudin–Shapiro sequence (dashed line), and the DNA human chromosome 22 – Ch22 (dotted line). Three values of the band fillings N_e/N are considered, namely (a) $N_e/N = 0.9$; (b) $N_e/N = 0.6$; (c) $N_e/N = 0.4$. The limit of the temperature scale (right-hand side) represents the normal human body temperature $T_{NHB} = 310$ K.

For small thermal excitations, each particle can absorb an energy of the order of T. The number of particles that can be excited corresponds to the number of states in an energy range of the order of T around the Fermi energy. Therefore, the observed specific heat exponents ϕ lies within the range of values of the singularity strength exponent $(\alpha_{min}, \alpha_{max})$ defined by the so-called multifractal $f(\alpha)$ spectrum [39], which in turn gives support to the above scaling analysis, unveiling a relationship between the low-temperature power-law decay of the ESH of a molecular system with multifractal spectrum and the underlying energy distribution singularities, disregarding the values of N_e/N and, of course, any finite size effect. This finding may provide a useful tool for the analysis of the low-temperature thermodynamic behavior of more robust protein models modeled by a quasiperiodic system.

There are some other features in the temperature dependence of the specific heat that deserve to be stressed:

(a) For the high temperature limit ($T \to \infty$), the specific heat for all sequences converges and decays as the power law T^{-2}. It is an expected result since the systems are considered bounded.
(b) At temperatures around the normal human being temperature $T_{NHB} = 310$ K a striking difference is observed: while the ESH for the Fibonacci sequence shows a peak, regardless the value of the band filling N_e/N, the same do not occur for the RS and Ch22, which have similar behavior.
(c) The RS and Ch22 structures show a peak at the temperature around 100 K with similar profiles.
(d) At low temperature the ESH falls linearly to zero, faster for the Fibonacci sequence than for the Rudin–Shapiro one, which in turn is faster than the DNA human chromosome 22.

In conclusion, we have presented in this Letter a theoretical model to study the electrons' specific heat spectra of an extended ladder model, made up from the nucleotides G, A, C, and T, arranged to form two artificial sequences, the Fibonacci and Rudin–Shapiro sequences, both with long-range correlations. We consider also the sequence of natural DNA as part of the human chromosome Ch22. For all structures studied in this work the oscillatory profile occurs in the low temperature region. They depend also on the type and the size of the sequence used to model the DNA molecule. Note also that the specific heat properties in log scale were basically controlled by the behavior of the low energy region at the scale considered, i.e., each oscillation can be thought as a change of scale in the spectrum. Besides, it is worth to mention the strike differences in the ESH profiles at the normal human body temperature $T_{NHB} = 310$ K.

In the experimental side, heat changes produced by protein unfolding, protein association, ligand binding, and other biological molecules reactions can now be measured routinely. The two principal instrument modes are the differential scanning calorimetry (DSC), which measures sample heat capacity with respect to a reference as a function of temperature, and isothermal titration calorimetry (ITC), which measures the heat uptake/evolution during a titration experiment (for a good description of them see the review Ref. [40]). The third major tool is a thermodynamic calorimetry. Unfortunately, none of these techniques is able to probe directly the electronic contribution to the specific heat of biological molecules: they encompass all contributions, including the vibrational one. Nevertheless, the theoretical predictions shown here can be tested experimentally, at least at the important low-temperature regime, considering these apparatus tools at the disposal of biophysicists and biochemists, and we expect that they will be motivated by our work to face them.

Acknowledgements

This work was partially financed by the Brazilian Research Agencies CAPES (PROCAD and Rede NanoBioTec), CNPq (INCT-Nano(Bio)Simes, Project No. 573925/2008-9) and FAPERN/CNPq (Pronex).

References

[1] C. Dekker, M. Ratner, Phys. World 14 (2001) 29.
[2] K.H. Yoo, et al., Phys. Rev. Lett. 87 (2001) 198102.
[3] S. Roche, D. Bicout, E. Maciá, E. Kats, Phys. Rev. Lett. 91 (2003) 228101; S. Roche, D. Bicout, E. Maciá, E. Kats, Phys. Rev. Lett. 92 (2004) 109901.
[4] M. Taniguchi, T. Kawai, Phys. Rev. E 70 (2004) 011913.

[5] R. Gutierrez, S. Mandal, G. Cuniberti, Nano Lett. 5 (2005) 1093.
[6] E. Maciá, S. Roche, Nanotechnology 17 (2006) 3002.
[7] A.V. Malyshev, Phys. Rev. Lett. 98 (2007) 096801.
[8] R.G. Sarmento, E.L. Albuquerque, P.D. Session Jr., U.L. Fulco, B.P.W. de Oliveira, Phys. Lett. A 373 (2009) 1486.
[9] L.M. Bezerril, D.A. Moreira, E.L. Albuquerque, U.L. Fulco, E.L. de Oliveira, J.S. de Sousa, Phys. Lett. A 373 (2009) 3381.
[10] R.G. Sarmento, U.L. Fulco, E.L. Albuquerque, E.W.S. Caetano, V.N. Freire, Phys. Lett. A 375 (2011) 3993.
[11] I. Jakli, A. Perczel, O. Farkas, A.G. Csaszar, C. Sosa, I.G. Csizmadia, J. Comput. Chem. 21 (2000) 626.
[12] S.M. Butterfield, P.R. Patel, M.L. Waters, J. Am. Chem. Soc. 124 (2002) 9751.
[13] M. Aida, G. Corongiu, E. Clementi, Int. J. Quantum Chem. 42 (1992) 1353.
[14] M.C. Payne, M.P. Teter, D.C. Allan, T.A. Arias, J.D. Joannopoulos, Rev. Mod. Phys. 64 (1992) 1045.
[15] P. Hohenberg, W. Kohn, Phys. Rev. B 136 (1964) 864.
[16] W. Kohn, L.J. Sham, Phys. Rev. A 140 (1965) 1133.
[17] R. Car, M. Parrinello, Phys. Rev. Lett. 55 (1985) 2471.
[18] G.A. Mendes, E.L. Albuquerque, U.L. Fulco, L.M. Bezerril, E.W.S. Caetano, V.N. Freire, Chem. Phys. Lett., in press.
[19] M. Zilly, O. Ujsághy, D.E. Wolf, Phys. Rev. B 82 (2010) 125125.
[20] B. Xu, P. Zhang, X. Li, N. Tao, Nano Lett. 4 (2004) 1105.
[21] J. Hihath, B. Xu, P. Zhang, N. Tao, Proc. Natl. Acad. Sci. USA 102 (2005) 16979.
[22] J. Hihath, F. Chen, P. Zhang, N. Tao, J. Phys.: Condens. Matter 19 (2007) 215202.
[23] E. Maciá, Rep. Prog. Phys. 69 (2006) 397.
[24] G. Cuniberti, E. Maciá, A. Rodriguez, R.A. Römer, in: T. Chakraborty (Ed.), Charge Migration in DNA: Perspectives from Physics, Chemistry and Biology, NanoScience and Technology, Springer, Berlin, 2007, Chap. 1.
[25] J.H. Wei, K.S. Chan, J. Phys.: Condens. Matter 19 (2007) 286101.
[26] D.A. Moreira, E.L. Albuquerque, D.H.L. Anselmo, Phys. Lett. A 372 (2008) 5233.
[27] K. Senthilkumar, F.C. Grozema, C.F. Guerra, F.M. Bickelhaupt, F.D. Lewis, Y.A. Berlim, M.A. Ratner, L.D.A. Siebbeles, J. Am. Chem. Soc. 127 (2005) 14894.
[28] T. Kubar, P.B. Woiczikowski, G. Cuniberti, M. Elstner, J. Phys. Chem. B 112 (2008) 7937.
[29] H. Zhang, X.-Q. Li, P. Han, X.Y. Yu, Y. Yan, J. Chem. Phys. 117 (2002) 4578.
[30] F. Axel, J.P. Allouche, Z.Y. Wen, J. Phys. Condens. Matter 4 (1992) 8713.
[31] E.L. Albuquerque, M.G. Cottam, Phys. Rep. 376 (2003) 225.
[32] E.L. Albuquerque, M.G. Cottam, Polaritons in Periodic and Quasiperiodic Structures, Elsevier, Amsterdam, 2004.
[33] M. Dulea, M. Johansson, R. Riklund, Phys. Rev. B 45 (1992) 105;
M. Dulea, M. Johansson, R. Riklund, Phys. Rev. B 46 (1992) 3296;
M. Dulea, M. Johansson, R. Riklund, Phys. Rev. B 47 (1993) 8547.
[34] H. Aynaou, V.R. Velasco, A. Nougaoui, E.H. El Boudouti, B. Djafari-Rouhani, D. Bria, Surf. Sci. 538 (2003) 101.
[35] A.-M. Guo, S.-J. Xiong, Phys. Rev. E 79 (2009) 041924.
[36] P. Dean, Rev. Mod. Phys. 44 (1972) 127.
[37] L.R. da Silva, R.O. Vallejos, C. Tsallis, R.S. Mendes, S. Roux, Phys. Rev. E 64 (2001) 11104.
[38] E. Schrödinger, What is Life? The Physical Aspect of the Living Cell, Cambridge University Press, Cambridge, 1945.
[39] D.H.A.L. Anselmo, A.L. Dantas, E.L. Albuquerque, Physica A 362 (2006) 289.
[40] I. Jelesarov, H.R. Bosshard, J. Mol. Recognit. 12 (1999) 3.